14-3-3σ Controls Corneal Epithelium Homeostasis and Wound Healing

Qingxian Lu,[1,2,3] *Ying Xin,*[1,2] *Fei Ye,*[2] *Gary Foulks,*[2] *and Qiutang Li*[1,2,3]

Purpose. To investigate the functional role of 14-3-3σ in regulation of the corneal epithelial proliferation, differentiation, and wound-healing response.

Methods. Corneal phenotypes were investigated in heterozygous repeated epilation (*Er*) mice carrying mutations in the *sfn* (14-3-3σ) gene. Immunohistochemistry was used to study the corneal morphogenesis of the *Er/Er* embryos at embryonic day (E)18.5. Corneal homeostasis and the wound-healing response were investigated macroscopically and microscopically in the adult heterozygous *Er* mice. Corneal epithelial cell proliferation and differentiation were assessed by BrdU incorporation and immunohistochemistry with specific antibodies for differentiation markers. Furthermore, corneal stroma neovascularization and meibomian gland degeneration were examined by immunohistochemistry. The healing of corneal wounds after debridement was monitored and visualized by fluorescent staining.

Results. Homozygous mutation of 14-3-3σ led to defects in embryonic corneal epithelial development and differentiation, whereas young heterozygotes showed normal corneal development and homeostasis. However, older heterozygotes displayed a dramatic corneal wound-healing defect characterized by hyperplastic basal progenitor cells (some of which undergo a differentiation switch to express markers of keratinized epidermis); cornea stroma changes including neovascularization; and corneal opacity, leading to plaque formation. Aged heterozygotes also showed meibomian gland atrophy.

Conclusions. 14-3-3σ is essential for corneal epithelium differentiation, and plays an important role in corneal epithelium development and daily renewal of the adult corneal epithelium. (*Invest Ophthalmol Vis Sci.* 2011;52:2389–2396) DOI:10.1167/iovs.09-4981

The corneal epithelium protects the eye from environmental injury. Cornea-related diseases are the second major cause of blindness after cataract. Loss of vision occurs primarily from corneal scarring and vascularization.[1] Vitamin A deficiency causes xerophthalmia, which is still a leading cause of childhood blindness due to corneal opacity associated with neovascularization. Because the corneal epithelium completely turns over every 7 to 10 days, there is ongoing corneal epithelial differentiation from proliferative progenitor cells scattered throughout the corneal epithelium and from the stem cells concentrated in the limbal region.[2–4] Progenitor cells in the basal layer divide and migrate gradually to the upper epithelial layer. During this process, the cells switch expression of cytokeratins from the progenitor markers keratin-5 (K5) and -14 (K14) to the differentiation-specific isoforms keratin-3 (K3) and -12 (K12).[5] The differentiated cells in the superficial layer then form tight junctions, which function as a barrier to protect the cornea.[6,7] After injury, the corneal epithelium is rapidly repopulated via a wound-healing process involving mobilization of the corneal stem cells. This wound-healing process is composed of three sequential and partially overlapping steps including cell migration, proliferation, and differentiation.[8,9]

14-3-3σ is essential for skin epithelial differentiation,[10,11] as demonstrated by the studies on the repeated epilation (*Er*) mouse that carries a null mutation in 14-3-3σ. 14-3-3σ is unique among seven 14-3-3 isoforms, which act exclusively as homodimers and are able to suppress tumor formation, and its expression is restricted to stratified squamous epithelial cells. It is induced at the transition from basal progenitor cells to suprabasal cells during the epidermal keratinocyte differentiation.[10,12] 14-3-3σ expression has been confined to corneal and conjunctival epithelial cells in humans and is secreted into the culture medium from either primary cells or cell lines.[13] In this report, we show that mice mutant for both copies of 14-3-3σ are defective in embryonic corneal development. Although the heterozygous mice exhibit normal corneal development and epithelial homeostasis during embryonic and early postnatal development, they develop an age-dependent corneal plaque formation associated with corneal epithelial wound-healing dysfunction and meibomian gland atrophy.

Materials and Methods

Animals

Er/+ mutant mice (mixed strain of C57BL/6J and CBA/CaGnLeJ) were originally purchased from the Jackson Laboratory (cat no. 000515; Bar Harbor ME). Experimental animals were housed under pathogen-free conditions and handled in accordance with the guidelines approved by the Institutional Animal Care and Use Committee (IACUC) of the University of Louisville. Animal management and the experimental protocols conformed to the ARVO Statement for the Use of Animals in Ophthalmic and Vision Research.

Tissue Collection

The embryos at E18.5 were harvested and fixed in 4% paraformaldehyde (PFA) at 4°C for 24 hours and further processed for paraffin sectioning. The *Er/Er* mouse were recognized by distinct morphology and/or by Western blot to detect the mutant 14-3-3σ protein.[10] At least four E18.5 embryos in each group were examined. For examination of the adult corneal phenotypes, both wild-type (WT) and *Er/+* mice at the ages

From the [1]J. G. Brown Cancer Center, and the Departments of [2]Ophthalmology and Visual Sciences and [3]Biochemistry and Molecular Biology, University of Louisville School of Medicine, Louisville, Kentucky.

Supported by National Center for Research Resources Grants RR018733; National Eye Institute grants R01-EY019891, EY018830, and EY015636 and by Research to Prevent Blindness, Inc., New York, New York.

Submitted for publication November 25, 2009; revised July 2 and October 18, 2010; accepted December 5, 2010.

Disclosure: **Q. Lu**, None; **Y. Xin**, None; **F. Ye**, None; **G. Foulks**, None; **Q. Li**, None

Corresponding author: Qiutang Li, Department of Ophthalmology and Visual Sciences, University of Louisville, 301 East Muhammad Ali Boulevard, Louisville, KY40202; q.li@louisville.edu.

of 1, 4.5, 6, and 7 months were intracardially perfused with 4% PFA. At least three animals from each group were analyzed, and the aged *Er/+* mice were separated to two groups, with or without visible plaques. The eyes were collected and further fixed in 4% PFA for 24 hours at 4°C, then dehydrated, paraffin-embedded, and serially sectioned at 7 μm. The three selected sections from each sample were stained with hematoxylin and eosin (H&E) for routine histologic examination.

Sudan Black Staining

For Sudan black staining, mice at ages of 1 and 4.5 months were intracardially perfused with 4% PFA, and the whole eyes, including the eyelids, were collected and fixed in 4% PFA at 4°C overnight and further treated with 20% sucrose/1× PBS for 24 hours at 4°C before being embedded in OCT and serially sectioned at 10 μm. Sudan black staining was performed as described. After a quick rinse in 50% ethanol (EtOH; 30 seconds), the eyelid sections were stained for 15 minutes in the saturated Sudan black B (cat. no. S2380; Sigma-Aldrich)/50% EtOH. After the sections were rinsed in 50% EtOH and in water, they were counterstained with Mayer's hematoxylin. The slides were mounted with PBS/glycerol and photographed by microscope.

Corneal Epithelial Wound-Healing and Corneal Fluorescein Staining

Three mice from each group of the *Er/+* or WT mice at the ages of 1, 3, 4.5, and 7 months were selected and anesthetized with an intraperitoneal injection of ketamine (50 mg/kg) and xylazine (5 mg/kg). After a few drops of topical 0.5% proparacaine were applied, the central epithelium within a cycle of 1.5-mm in diameter and exclusion of the limbal area was demarcated and removed by gentle scraping. The epithelial wounding was monitored right after injury by the fluorescein staining. Corneal surface integrity was examined and photographed with a slit lamp biomicroscope equipped with a cobalt blue light, after a 2-minute surface staining with 2 μL of 0.5% fluorescein sodium salt and intense washout of the extra fluorescein with 1× PBS.[14] The wound-healing process after 24 and 48 hours of wounding were further monitored and recorded using the fluorescein staining method described earlier.

Immunohistological Analysis

Whole eyes were fixed in 4% PFA at 4°C overnight and processed for paraffin embedding, with sagittal sections subsequently cut at 7 μm. For most of the fluorescence labeling, the slides were deparaffinized and retrieved for antigen detection in Tris-EDTA buffer (for 1 L: 1.2 g Tris and 0.37 g EDTA [pH 9.0]) for 20 minutes at 95°C, followed by slow cooling to room temperature in a warm container.

The nonspecific background was blocked in 1× blocking buffer (1× PBS, 0.2% Triton X-100, 5% normal serum) for 1 hour at room temperature (RT). The sections were then labeled with the primary antibodies for 90 minutes at RT. For negative controls, the sections were incubated with an irrelevant (no epithelial expression of the antigen) antibody or without the primary antibody. The fluorescein-conjugated secondary antibodies were incubated for 1 hour at RT.

The following antibodies were used for immunostaining: rabbit anti-K10 (1:500, PRB-145P), rabbit anti-K14 (1:500, PRB-145P) antibodies were purchased from Covance Research Products (Denver, PA), and mouse anti-p63 (1:200, sc-8431), goat anti-C terminus of 14-3-3σ (1:200, sc-7683), and goat anti-K12 (1:200, sc-17101) antibodies were from Santa Cruz Biotechnology (Santa Cruz, CA). Additional antibodies included rat anti-BrdU (1:800, MAS 250c; Harlan-Sera Laboratory, North Loughborough, UK) and rat anti-CD31 (1:200, cat no. 550274; BD Biosciences, Franklin Lakes, NJ). Secondary Cy3 and FITC-conjugated antibodies were obtained from Jackson ImmunoResearch Laboratories, Inc. (West Grove, PA). Nuclei were stained by diamidinophenylindole (DAPI).

For BrdU labeling of the proliferating cells, the mice were injected with 5-bromo-2′-deoxyuridine [BrdU]; 150 mg/kg body weight) for 90 minutes before death. Cornea sections, as prepared for fluorescent staining, were denatured for 30 minutes with 2 N HCl. After neutralization, the sections were incubated with a specific rat anti-BrdU antibody, followed by a regular immunostaining procedure.

BrdU- and K14-Positive Cell Counts and Statistical Analysis

In each section, the BrdU- and K14-positive cells, as well as the total number of cells as shown by DAPI nuclear staining, were counted on a digital micrograph taken at 32× magnification. The percentage of the BrdU- or K14-labeled cells in the total cornea epithelial cells (~1000 cells) as labeled by DAPI was calculated based on results of counts in six sections from three mice in each experimental group. We also counted the average number of BrdU- or K14-positive cells in a defined length of corneal epithelium from at least six sections of each group. All data are shown as the average ± SD. The differences were considered statistically significant at $P < 0.05$.

Western Blot Analysis

Corneas were isolated from WT and plaqued Er/+ eyes prepared from 7-month-old mice under a dissecting microscope and were homogenized in cold RIPA buffer plus protease inhibitor cocktail tablet (Roche, Indianapolis, IN). Equal amounts of cell lysates were separated on 10% SDS-polyacrylamide gel and transferred to a nitrocellulose membrane. After incubation in blocking buffer (10 mM Tris [pH 8.0], 150 mM NaCl, and 0.1% Tween-20 [TBST], in 5% nonfat milk) for 30 minutes at RT, the blots were incubated with primary antibodies in blocking buffer at RT for 2 hours. The primary antibodies used included mouse anti-p63 (1:100, cat no. sc-8431), goat anti-14-3-3σ (1:100, cat no. sc-7681), goat anti-K12 (1:100, cat no. sc-17,101), and goat anti-Notch 1 (1:100, cat no. sc-23304) antibodies from Santa Cruz Biotechnology (Santa Cruz, CA); rabbit anti-K14 (1:500, cat no. PRB-145P; Covance Research Products); mouse anti-PCNA (1:100, cat no. 180110; Invitrogen, Carlsbad, CA), and mouse anti-β-actin (1:1000, cat no. A2228; Sigma-Aldrich) antibodies. By the end of incubation, the membranes were washed three times with TBST before incubation for 30 minutes at RT with the appropriate secondary antibodies conjugated to horseradish peroxidase (GE Healthcare. Piscataway, NJ) in blocking buffer. After three washes with TBST, the blots were visualized with an enhanced chemiluminescence (ECL) system (GE Healthcare).

Results

Corneal Morphogenesis and Differentiation Are Impaired in *Er/Er* Mice

Er mice carrying a null mutation in 14-3-3σ showed impaired differentiation of the skin epithelium, as characterized by accumulation of proliferating progenitor cells.[10,11] Because of its role in skin epithelial differentiation, we wondered whether 14-3-3σ was also important for corneal epithelial differentiation in the eye. Although *Er/Er* embryos formed a normal lens and retina, corneal and conjunctival epithelial differentiation was abnormal. E18.5 embryos displayed a fused conjunctival sac, which was never fully separated into conjunctival and corneal epithelial layers (Figs. 1A, 1B). These progenitor cells expressed 14-3-3σ, suggesting a role for the protein in embryonic corneal formation (Fig. 1C). K14 was expressed by undifferentiated basal cells throughout the corneal, conjunctival, and epidermal epithelia (Fig. 1D, a, b, c, respectively). In contrast to the well-separated single cell layer of K14-positive cells in the WT conjunctival and corneal epithelia, *Er/Er* eyes showed a single multilayered K14-positive cell strip that failed to segregate into conjunctival and corneal epithelia (Fig. 1E, b, c). Consistent with the previously documented role of 14-3-3σ in epidermal differentiation, accumulation of an expanded K14-positive epidermal layer was evident on the surface of the eyelid.

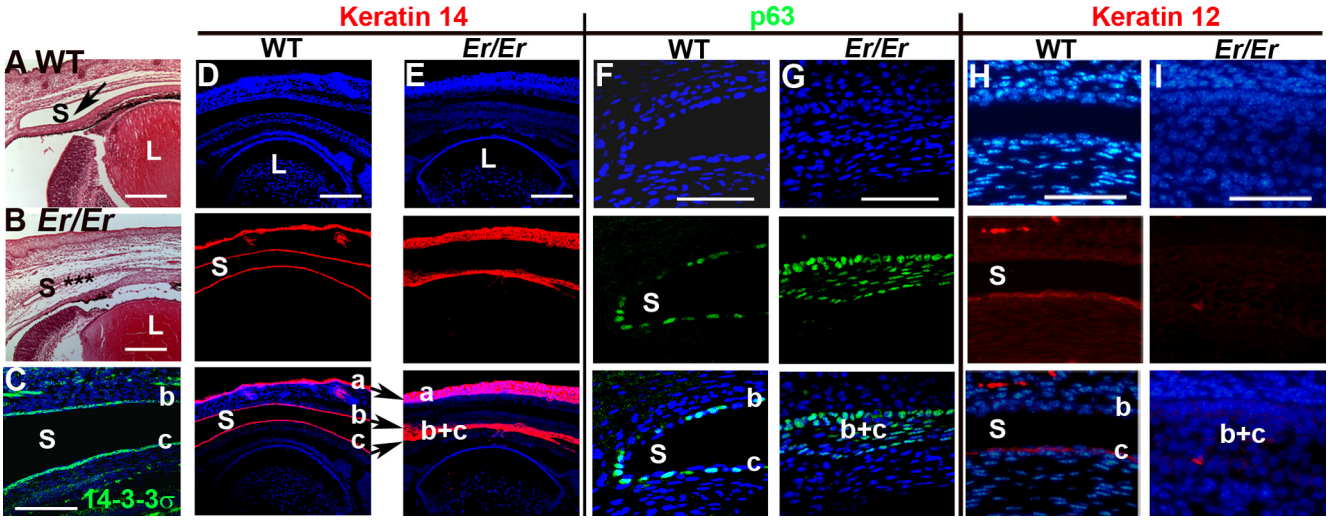

Figure 1. Corneal defects in *Er/Er* mice at E18.5. (**A**, **B**) H&E staining of sagittal sections of WT and *Er/Er* corneas from E18.5 embryos. *Arrow*: the conjunctival sac (S) in the WT eye (**A**); (✱) the unseparated conjunctival sac in the *Er/Er* eye (**B**). (**C**) Immunostaining for14-3-3σ was evident on both conjunctival (b) and corneal (c) epithelial cells. (**D**, **E**) K14 immunostaining (*red*) was restricted to basal cells of epidermal (a), conjunctival (b), and corneal (c) epithelia in the WT control (**D**), but expanded in the skin epidermal layer (a), and the conjunctival sac failed to separate into conjunctival and cornea epithelia (b, c) in the *Er/Er* mice (**E**). (**F**, **G**) p63 (*green*) was normally restricted to the conjunctival basal progenitor cells, which line the single layer of conjunctival and corneal epithelial cells (**F**), but the conjunctival sac in the *Er/Er* mice was not completely formed, and it filled with the expanded p63-positive cells (**G**). The corneal epithelial marker, K12 was labeled *red* in the WT (**H**), but not in the *Er/Er* (**I**) corneas. *Top*: nuclei counterstained with DAPI; *middle*: antibody staining; *bottom*: merged images. L, lens. Small letters mark skin (a), conjunctival (b), and corneal (c) epithelia. (b, c) The unseparated conjunctival and corneal epithelial fusion. Scale bars: (**A–E**) 100 μm; (**F–I**) 50 μm.

p63, an epithelial progenitor marker that is downregulated during differentiation, immunostained positively on both conjunctival and corneal epithelial cells, which lined the conjunctival sac in the E18.5 WT eye (Fig. 1F, b, c). However, the p63-positive cells in the *Er/Er* mutant eye occupied an entire region that normally differentiated into the conjunctival sac (Fig. 1G). K12 keratin, a central cornea epithelial cell differentiation marker, expressed in the WT cornea epithelium but lost in *Er/Er* corneal epithelium (Figs. 1H, 1I). Thus, as in the skin, homozygous mutation of 14-3-3σ led to a block in corneal epithelial differentiation with accumulation of proliferating progenitor cells.

Mice Heterozygous for 14-3-3σ Show Normal Corneal Epithelial Development and Postnatal Homeostasis, but Develop Corneal Plaques as They Age

Er/Er homozygous mice die at birth, precluding further studies of the role of the 14-3-3σ in homozygous mutant mice. How-

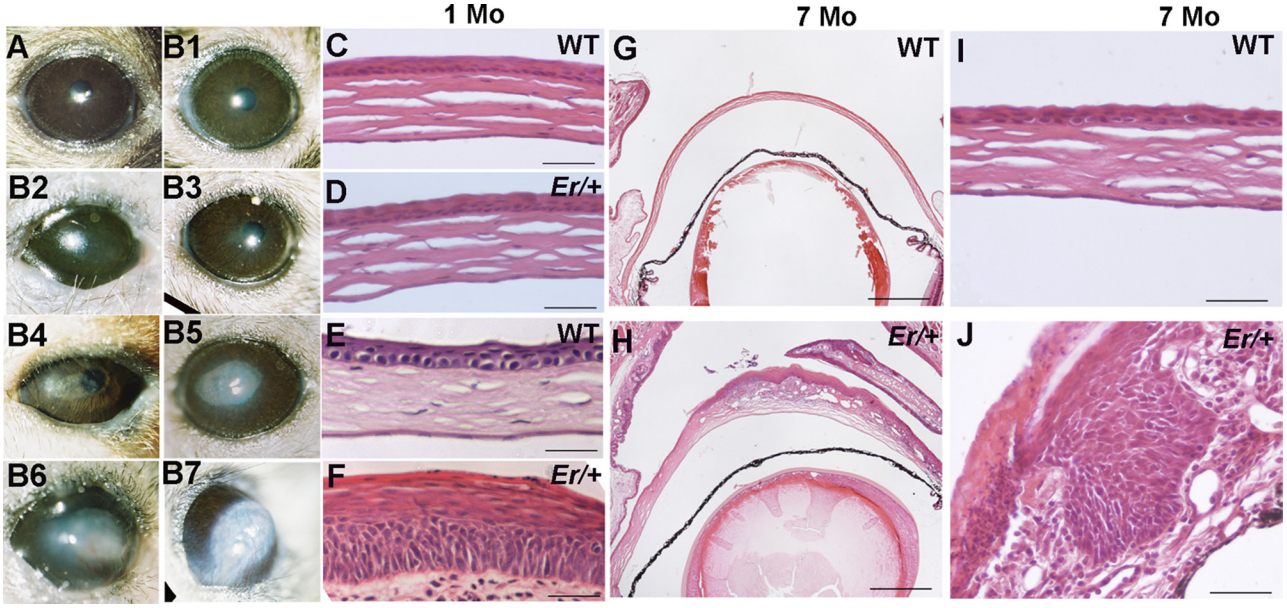

Figure 2. *Er/+* mice spontaneously developed aging-related plaques on the central corneal surface. Corneal light macrographs were taken of the 7-month-old WT mice (**A**) and the *Er/+* mice at the ages of 1 (**B1**), 4.5 (**B2**, **B3**), 6 (**B4**, **B5**), and 7 (**B6**, **B7**) month. Light microscopy of H&E-stained corneal sections of WT (**C**, **E**, **G**, **I**) and *Er/+* (**D**, **F**, **H**, **J**) mice at the ages of 1 (**C**, **D**), 6 (**E**, **F**), and 7 (**G–J**) months are presented. (**G**, **H**) Low-magnification views (40×); (**I** , **J**) high-magnification views (×400). Scale bars: (**C–F**, **I–J**) 50 μm; (**G**, **H**) 500 μm.

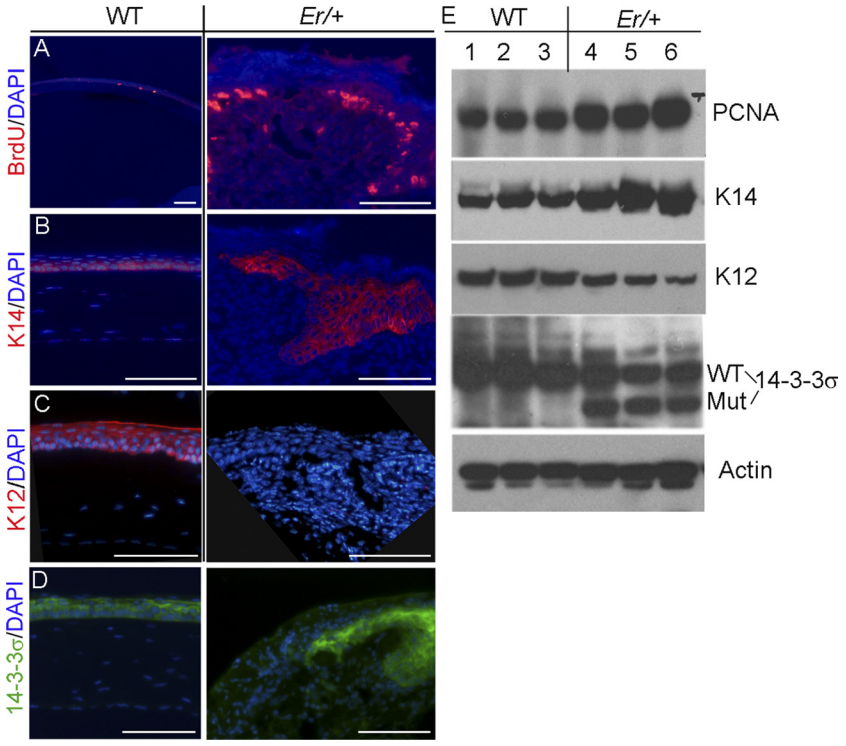

Figure 3. Cells in corneal epithelial plaques were hyperproliferative and abnormally differentiated. (**A**) Corneal sections from 7-month-old WT (*left*) and plaque-containing *Er/+* (*right*) mice were stained for BrdU (*red*) incorporation. (**B**) K14 (*red*) was present in the basal corneal epithelium of the control mice, but expanded to the suprabasal layer in the *Er/+* animals. (**C**) The corneal epithelial differentiation marker, K12 was labeled *red* in the WT but not in the *Er/+* corneas. (**D**) 14-3-3σ expression (*green*) was detected in the corneal epithelium of the WT and the *Er/+* mice. Nuclei were stained *blue* with DAPI. Scale bars: 100 μm. (**E**) Western analyses WT and plaque-containing *Er/+* corneas. *Lanes 1–6*: the protein extracts of three WT and three plaque-containing *Er/+* corneas from 7-month-old mice.

ever, because the *Er/+* mice heterozygous for 14-3-3σ showed epidermal defects, we wondered whether mutation of a single copy of 14-3-3σ would also lead to defects in corneal epithelium. We did not detect any obvious defects in corneal development in the E18.5 embryos and in the corneal epithelium of the 14-3-3σ heterozygotes at 1 and 3 months of age, suggesting that a single copy of 14-3-3σ is sufficient for corneal development and corneal epithelial homeostasis in the young mice (Figs. 2A, 2B1, 2C, 2D). However, between 6 and 12 months of age, more than 50% of the *Er/+* mice developed central corneal opacity. The corneal haze was detectable in some heterozygous mice as early as 4.5 months of age (Figs. 2B2, 2B3), and these plaques increased in size with age (Figs. 2A, 2B1–B7). Histologic examination of the corneal plaques from the *Er/+* mice at the ages of 6 (Figs. 2E, 2E, 2F) and 7 (Figs. 2G–2J) months showed corneal epithelial hyperplasia and invasion to the underlying stroma.

Plaque Formation on the Cornea of *Er/+* Mice Is Associated with Increased Corneal Epithelial Proliferation and Block in Differentiation

We used BrdU incorporation as a measure of corneal epithelial proliferation. In WT mice, there were approximately 2% of the corneal epithelial cells labeled with BrdU within 90 minutes after intraperitoneal (IP) injection (Fig. 3A, left). BrdU incorporation was indistinguishable between the WT and the young *Er/+* mice at 3 months of age before plaque formation; however, a dramatic

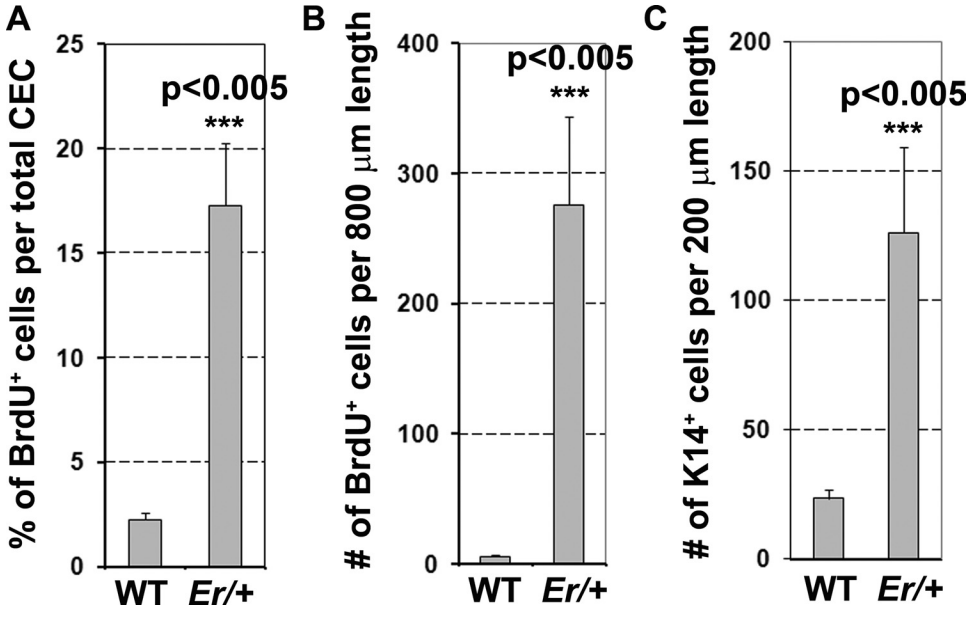

Figure 4. Quantification of $BrdU^+$ and K14-positive cells in the corneal epithelium of the WT and plaque-containing *Er/+* mice at 7 months of age. (**A**) Percentage of $BrdU^+$ cells in the total corneal epithelial cells (CECs). (**B**) The number of $BrdU^+$ cells per 800 μm of fixed length parallel to the cornea surface. (**C**) The number of the K14-positive cells per 200 μm of fixed length parallel to the corneal surface. Two-tailed *t*-test: $P < 0.005$; $n = 5$.

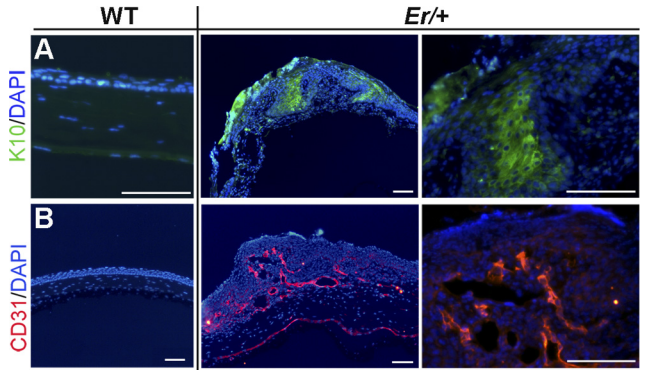

FIGURE 5. Corneal epithelium in the plaque-forming sites was keratinized and associated with stromal neovascularization. (**A**) Immunostaining for K10 (*green*) was evident in the corneas of 7-month-old plaque-containing *Er/+* mice but not in the corneas of the WT littermates, suggesting keratinization of the corneal epithelium in the plaque-forming region of the *Er/+* cornea. (**B**) Neovascularization in the *Er/+* stroma was visualized by immunostaining for CD31 (*red*), a marker for blood vessel endothelial cells. Nuclei were stained *blue* with DAPI. Scale bar, 100 μm.

increase in BrdU-positive cells occurred in the plaque-forming corneal epithelium as the *Er/+* mice aged (~17% of the cells incorporated BrdU; Fig. 3A, right). When counted within a fixed distance of 800 μm parallel to the corneal surface, the number of BrdU-positive cells increased to approximately 270 cells in the plaqued *Er/+* corneas from an average of 6 $BrdU^+$ cells in the WT corneas (Figs. 4A, 4B). To determine the differentiation status, we immunostained these proliferating cells with the basal cell marker K14 and the corneal epithelial differentiation marker K12. Most of the proliferating cells were K14-positive, but K12 was missing in the plaque-forming regions, suggesting that the cells were undifferentiated (Figs. 3B, 3C, 4C). We further validated these immunohistochemical results with Western blot analysis and demonstrated that the expressions of both proliferating cell nuclear antigen (PCNA), a cell-proliferation marker, and K14 were increased and the K12 level was reduced in the plaque-containing *Er/+* corneas (Fig. 3E).

Consistent with the defective phenotypes in the affected corneas, 14-3-3σ expression was evident in the WT corneal epithelium and persisted into adulthood (Fig. 3D). The *Er/+* mice carry one mutant 14-3-3σ allele, which expresses a truncated protein that has dominant negative functions,[10] and they also carry one normal allele expressing the WT 14-3-3σ protein that can be recognized with the antibody specifically against the C terminus of the full-length protein. Notably, the 14-3-3σ was indeed detected in the plaques on the *Er/+* corneas (Fig. 3D, right), consistent with the notion that a block in cell cycle arrest and differentiation occurs at the point in the differentiation process when 14-3-3σ is expressed.

The Corneal Plaque in *Er/+* Mice Is Keratinized

In contrast to epidermal epithelium, the WT corneal epithelial cells were not keratinized and did not express the epidermal cell–specific marker K10, but instead, expressed the cornea-specific K12. However, to our surprise, patches of cells in the *Er/+* corneal plaques expressed the epidermal cell–specific K10 (Fig. 5A), which was normally not expressed by the corneal epithelial cells in the WT mice or in the *Er/+* mice before plaque formation. Taken together, our results demonstrate that there is an increase in the proliferating and undifferentiated progenitor cells in the plaques, which express both 14-3-3σ and K14. Some of the cells in the plaques are undergoing differentiation, but the differentiation is aberrant and appears to represent a keratinized phenotype.

Plaque Formation Is Associated with Stromal Remodeling and Neovascularization

The stroma underlying the corneal epithelium is normally avascular, which is essential for maintaining visual acuity and is organized in arrays of flattened cells parallel to the epithelial surface (Fig. 5, left). After corneal injury, the stroma can undergo transition to myofibroblastic cells resembling the stellate-shaped cells resulting from the epithelial–mesenchymal transition during fibrotic disease.[15] Proliferating epithelial progenitors in the plaques invaded the corneal stroma layer, leading to disorganization of the stromal arrays. Immunostaining for the endothelial marker CD31 demonstrated that this invasion into the stroma was accompanied by neovascularization (Fig. 5B). We did not detect 14-3-3σ expression in the stroma or in the newly formed vessels in the plaques; therefore, the corneal neovascularization is probably a secondary event initiated by the invading epithelial progenitors.

Corneal Wounding Initiates an Age-Dependent Abnormal Wound-Healing Response in *Er/+* Mice

Recent studies showed that the Notch signaling pathway plays a key role in epithelial differentiation, mutation in Notch 1 led to age-dependent plaque formation that resulted from abnormal wound-healing response in the affected mouse cornea.[16] The phenotypes in the Notch1-mutated cornea closely resemble what we found in the 14-3-3σ heterozygous mice, and we recently showed that 14-3-3σ regulates corneal epithelial cell differentiation through Notch signaling in cell culture. We therefore wondered whether plaque formation in the 14-3-3σ heterozygous mice is also linked to the reduced Notch1 activity and abnormal healing. We examined the level of Notch intracellular domain (NICD), an activate form of Notch1, in the plaqued *Er/+* corneas by Western blot. As expected, a significant reduction in NICD level was detected in the plaque-containing *Er/+* corneas (Fig. 6). In contrast, p63, a proliferation promoter and a Notch1-suppressing target,[17] was increased

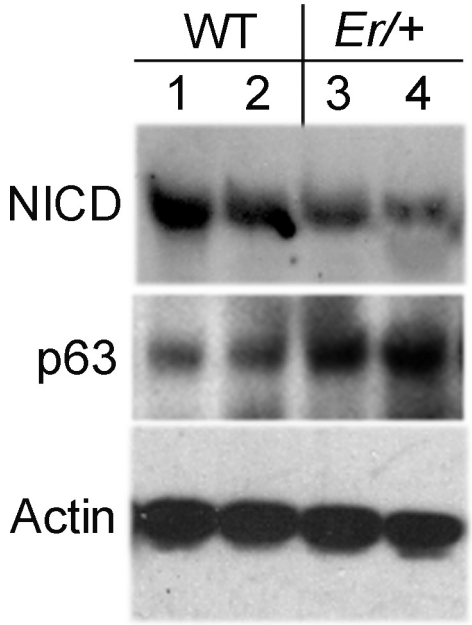

FIGURE 6. NICD activity was downregulated and p63 was upregulated in the plaque-containing *Er/+* corneas, according to Western blot analysis. *Lanes 1–4*: the protein extracts of two WT and two plaque-containing *Er/+* corneas from 7-month-old mice.

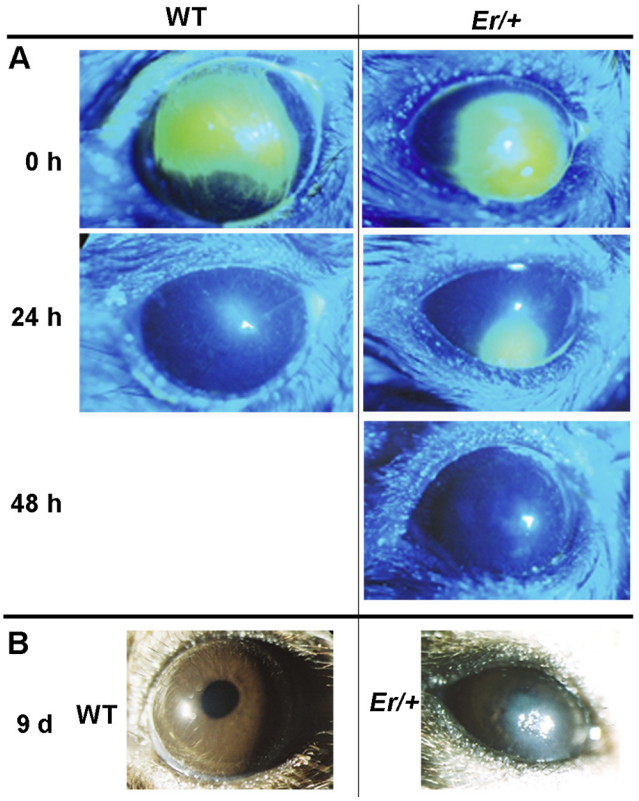

FIGURE 7. Corneal wounding initiated abnormal wound-healing response in *Er/+* mice. (**A**) Wound-healing was assayed on the corneal surface of the younger WT (*left*) and the *Er/+* mice (*right*) at the ages of 4.5 months. The fluorescein-stained eye images were taken under cobalt-filtered ultraviolet light at 24 and 48 hours after mechanical scraping of the center corneal epithelium. (**B**) Wounding healing was monitored on the corneal surface of the WT (*left*) and *Er/+* mice (*right*) at the age of 7 months for 9 days, and the images were taken at day 9 after corneal injury.

in the plaqued *Er/+* corneas (Fig. 6). The *Er/+* corneas were then wounded before plaque formation at the ages of 1.0, 3.0, 4.5, and 7.0 months, as described.[18] The epithelial wound was observed and monitored with fluorescein dye. While both WT (Fig. 7A, left) and the young *Er/+* mice at the ages of 1- and 3- months completely recovered at 24 hours after wounding, as evidenced by dye exclusion, the corneas in the *Er/+* mice at the age of 4.5 months showed a delay in healing (dye-stained lesions remained evident for 48 hours under the same conditions), but the wound eventually appeared to heal (Fig. 7A, right). Of interest, older mice at 7 months of age all developed corneal plaques after wounding (Fig. 7B), and the plaques were histologically indistinguishable from those arising spontaneously in the mice. Taken together, these results demonstrate that wounding initiates plaque formation in *Er/+* mice in an age-dependent process.

Meibomian Gland Atrophy in 14-3-3σ Heterozygous Mice

We then wondered whether spontaneous plaque formation in the 14-3-3σ heterozygous mouse is associated with meibomian gland atrophy, as it is in *Notch1* mutant mice. Therefore, we examined the meibomian glands of *Er/+* mice at 1.0 and 4.5 months of age histologically. The glandular atrophy with reduced lipid contents was pronounced by 4.5 months of age (Fig. 8A). Note that 14-3-3σ was strongly expressed in the suprabasal cells in the ductal epithelium of the meibomian gland, but not in the acinar cells (Fig. 8B).

DISCUSSION

In the present study, 14-3-3σ was crucial for corneal epithelial differentiation. Homozygous mutation of 14-3-3σ led to defects in embryonic corneal epithelial development, whereas young heterozygotes showed normal corneal development and corneal epithelial homeostasis. However, as the heterozygous mice aged, they developed corneal surface opacity. Corneal wounding of the old 14-3-3σ heterozygotes triggered a similar corneal plaque formation phenotype. We also found that the meibomian glands appeared atrophic in the aged *Er/+* mice and that 14-3-3σ was expressed in the stratified squamous ductal epithelium of the gland but not in the acinar cells. The ductal epithelium consists of a basal cell layer, an intermediate layer, and a superficial horny cell layer. The suprabasal layer is keratinized. Hyperkeratinization of the meibomian ductal gland is associated with the development of meibomian gland dysfunction (MGD) in humans and animals.[19] The abnormal keratinization in the

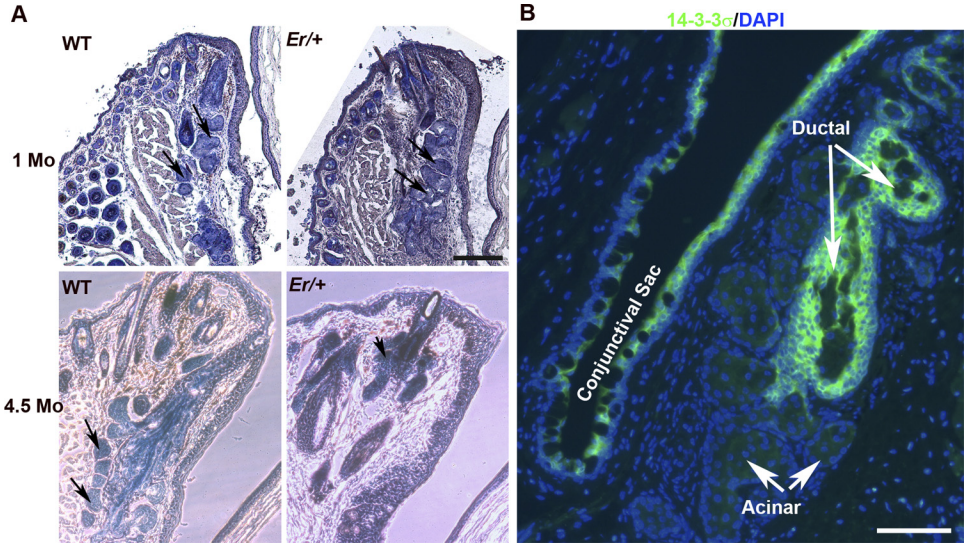

FIGURE 8. Aged *Er/+* mice showed evidence of meibomian gland atrophy. (**A**) Lipids in meibomian glands were stained with Sudan black (*blue*), and the slides were counterstained with H&E. Eye sections of WT and *Er/+* mice at 1.0 and 4.5 months of age are shown. The images representative of serial sections through the glands. *Arrows*: sebaceous glands. (**B**) Immunostaining for 14-3-3σ (*green*) in a WT eye section containing sebaceous glands. The nuclei were counterstained with DAPI. Scale bar, 100 μm.

rhino mouse is believed to cause the plugging of the meibomian gland orifice and then the atrophy of the entire meibomian gland.[20] It is possible that, as evident in the corneal epithelial plaques, reduced 14-3-3σ activity also leads to hyperkeratinization in the meibomian ductal cells. However, since the meibomian glands in the 14-3-3σ heterozygotes appeared to form normally and developed atrophy as the mice aged, it is also possible that such atrophy is caused by a failure to replace the meibomian gland ductal epithelium during normal epithelium renewal.

The corneal epithelial wound-healing abnormality and meibomian gland atrophy seen in the 14-3-3σ heterozygotes appears similar to that in the *Notch1* conditional knockout mice.[16] In response to wounding, basal progenitor cells in the conditional *Notch1* mutants became hyperplastic. Most of these cells failed to differentiate, and those that did showed evidence of a differentiation switch and expressed markers of keratinized epidermis. The proliferating progenitor cells invaded the corneal stroma, leading to stromal remodeling, neovascularization, and ultimately, corneal opacity. This corneal phenotype resembles vitamin A deficiency in mice, and Notch1 has been shown to be necessary for expression of RBP1, which is essential for vitamin A transportation and metabolism in the corneal epithelium.[16,21] Conditional knockout of *Notch1* also led to a defective meibomian gland. This gland normally secretes the lipid component of tears, and loss of a functional gland leads to dry eye.[16] The dry-eye phenotype associated with lack of meibomian gland function in the *Notch1* mutant mice spontaneously initiates an abnormal wound-healing response as the mutant mice age.[16] We demonstrated that the corneal epithelial cells with reduced 14-3-3σ activity due to the dominant negative effect of the Er mutant protein showed reduced Notch1/2 transcription and activity. Restoring Notch1 activity in the mutant cells rescued the differentiation-associated tight junction formation defect.[22] We speculate that 14-3-3σ could modulate Notch1 transcription by regulating cytoplasmic–nuclear translocation of transcription factors that control Notch1 transcription. It has been shown that cadherin-initiated junction formation initiates a kinase cascade known as Hippo, which phosphorylates a set of transcription factors, Yap and Taz.[23–25] This phosphorylation provides a binding site for 14-3-3, which causes Yap and Taz to be sequestered in an inactive form in the cytoplasm.[26–28] Mutations in components of the Hippo kinase cascade in *Drosophila* leads to loss of Notch1 activity.[29,30] It will be interesting in future studies to examine whether 14-3-3σ modulates Notch1 transcription through Yap/Taz.

Finally, 14-3-3σ is a tumor suppressor, and its expression is frequently epigenetically silenced in basal cell carcinoma, which is characterized by a failure of basal cell differentiation, leading to hyperplastic progenitors.[31,32] In this regard, it is of note that the invasive, hyperplastic progenitor phenotype that we observed in the corneal epithelial plaques in 14-3-3σ heterozygotes resembles early-stage cancer cells. Thus, it is interesting to consider the possibility that the age-related progression toward dependency on full 14-3-3σ activity in corneal epithelial differentiation may provide insight into why 14-3-3σ is a tumor suppressor in adult cancers. Loss of 14-3-3σ activity, as a result of epigenetic inhibition of expression, may facilitate generation of undifferentiated hyperplastic progenitors resembling early cancer cells in adult squamous epithelium as the tissues undergo normal homeostasis or wound repair.

Acknowledgments

The authors thank Doug Dean, John Gamel, and Guoming Jiang for valuable discussions.

References

1. Whitcher JP, Srinivasan M, Upadhyay MP. Corneal blindness: a global perspective. *Bull World Health Organ.* 2001;79:214–221.
2. Schermer A, Galvin S, Sun TT. Differentiation-related expression of a major 64K corneal keratin in vivo and in culture suggests limbal location of corneal epithelial stem cells. *J Cell Biol.* 1986;103:49–62.
3. Cotsarelis G, Cheng SZ, Dong G, Sun TT, Lavker RM. Existence of slow-cycling limbal epithelial basal cells that can be preferentially stimulated to proliferate: implications on epithelial stem cells. *Cell.* 1989;57:201–209.
4. Lavker RM, Tseng SC, Sun TT. Corneal epithelial stem cells at the limbus: looking at some old problems from a new angle. *Exp Eye Res.* 2004;78:433–446.
5. Wolosin JM, Budak MT, Akinci MA. Ocular surface epithelial and stem cell development. *Int J Dev Biol.* 2004;48:981–991.
6. Ban Y, Dota A, Cooper LJ, et al. Tight junction-related protein expression and distribution in human corneal epithelium. *Exp Eye Res.* 2003;76:663–669.
7. Sugrue SP, Zieske JD. ZO1 in corneal epithelium: association to the zonula occludens and adherens junctions. *Exp Eye Res.* 1997;64:11–20.
8. Lu L, Reinach PS, Kao WW. Corneal epithelial wound healing. *Exp Biol Med (Maywood).* 2001;226:653–664.
9. Suzuki K, Saito J, Yanai R, et al. Cell-matrix and cell-cell interactions during corneal epithelial wound healing. *Prog Retin Eye Res.* 2003;22:113–133.
10. Li Q, Lu Q, Estepa G, Verma IM. Identification of 14-3-3sigma mutation causing cutaneous abnormality in repeated-epilation mutant mouse. *Proc Natl Acad Sci U S A.* 2005;102:15977–15982.
11. Herron BJ, Liddell RA, Parker A, et al. A mutation in stratifin is responsible for the repeated epilation (Er) phenotype in mice. *Nat Genet.* 2005;37:1210–1212.
12. Xin Y, Lu Q, Li Q. 14-3-3sigma is required for club hair retention. *J Investig Dermatol.* 2010;130:1934–1936.
13. Shankardas J, Senchyna M, Dimitrijevich SD. Presence and distribution of 14-3-3 proteins in human ocular surface tissues. *Mol Vis.* 2008;14:2604–2615.
14. Rashid S, Jin Y, Ecoiffier T, Barabino S, Schaumberg DA, Dana MR. Topical omega-3 and omega-6 fatty acids for treatment of dry eye. *Arch Ophthalmol.* 2008;126:219–225.
15. Saika S, Yamanaka O, Sumioka T, et al. Fibrotic disorders in the eye: targets of gene therapy. *Prog Retin Eye Res.* 2008;27:177–196.
16. Vauclair S, Majo F, Durham AD, Ghyselinck NB, Barrandon Y, Radtke F. Corneal epithelial cell fate is maintained during repair by notch1 signaling via the regulation of vitamin A metabolism. *Dev Cell.* 2007;13:242–253.
17. Nguyen BC, Lefort K, Mandinova A, et al. Cross-regulation between notch and p63 in keratinocyte commitment to differentiation. *Genes Dev.* 2006;20:1028–1042.
18. Wilson SE, Mohan RR, Ambrosio R, Mohan RR. Corneal injury: a relatively pure model of stromal-epithelial interactions in wound healing. *Methods Mol Med.* 2003;78:67–81.
19. Jester JV, Rife L, Nii D, Luttrull JK, Wilson L, Smith RE. In vivo biomicroscopy and photography of meibomian glands in a rabbit model of meibomian gland dysfunction. *Invest Ophthalmol Vis Sci.* 1982;22:660–667.
20. Jester JV, Rajagopalan S, Rodrigues M. Meibomian gland changes in the rhino ($hr^{rh}hr^{rh}$) mouse. *Invest Ophthalmol Vis Sci.* 1988;29:1190–1194.
21. Ghyselinck NB, Bavik C, Sapin V, et al. Cellular retinol-binding protein I is essential for vitamin A homeostasis. *EMBO J.* 1999;18:4903–4914.
22. Xin Y, Lu Q, Li Q. 14-3-3sigma controls corneal epithelial cell proliferation and differentiation through the Notch signaling pathway. *Biochem Biophys Res Commun.* 2010;392:593–598.
23. McNeill H, Woodgett JR. When pathways collide: collaboration and connivance among signalling proteins in development. *Nat Rev Mol Cell Biol.* 2010;11:404–413.

24. Yin F, Pan D. Fat flies expanded the hippo pathway: a matter of size control. *Sci STKE.* 2007;2007:pe12.
25. Zhao B, Wei X, Li W, et al. Inactivation of YAP oncoprotein by the Hippo pathway is involved in cell contact inhibition and tissue growth control. *Genes Dev.* 2007;21:2747–2761.
26. Lei QY, Zhang H, Zhao B, et al. TAZ promotes cell proliferation and epithelial-mesenchymal transition and is inhibited by the hippo pathway. *Mol Cell Biol.* 2008;28:2426–2436.
27. Ren F, Zhang L, Jiang J. Hippo signaling regulates Yorkie nuclear localization and activity through 14-3-3 dependent and independent mechanisms. *Dev Biol.* 2010;337:303–312.
28. Kanai F, Marignani PA, Sarbassova D, et al. TAZ: a novel transcriptional co-activator regulated by interactions with 14-3-3 and PDZ domain proteins. *EMBO J.* 2000;19:6778–6791.
29. Polesello C, Tapon N. Salvador-warts-hippo signaling promotes Drosophila posterior follicle cell maturation downstream of notch. *Curr Biol.* 2007;17:1864–1870.
30. Yu J, Poulton J, Huang YC, Deng WM. The hippo pathway promotes Notch signaling in regulation of cell differentiation, proliferation, and oocyte polarity. *PLoS One.* 2008;3:e1761.
31. Lodygin D, Yazdi AS, Sander CA, Herzinger T, Hermeking H. Analysis of 14-3-3sigma expression in hyperproliferative skin diseases reveals selective loss associated with CpG-methylation in basal cell carcinoma. *Oncogene.* 2003;22:5519–5524.
32. Ferguson AT, Evron E, Umbricht CB, et al. High frequency of hypermethylation at the 14-3-3 sigma locus leads to gene silencing in breast cancer. *Proc Natl Acad Sci U S A.* 2000;97:6049–6054.